PERFORMANCE ANALYSIS OF BEAMFORMING FOR MIMO RADAR

Y. Qu [†]**, G. S. Liao, S. Q. Zhu, X. Y. Liu, and H. Jiang**

National Key Laboratory of Radar Signal Processing
Xidian University
Xi'an 710071, P. R. China

Abstract—The full MIMO radar and the partial MIMO one are introduced. The performance analysis of beamforming for MIMO (Multiple-input Multiple-output) radar and comparisons with the phased-array radar are given. The expressions of beamwidth, gain loss and detection range for MIMO radar are derived. Theoretical analysis and simulations show that the beam of the full MIMO utilizing all virtual array elements is identical to the two-way beam of the phased-array radar, and that the beam of the partial MIMO selecting elements with different phase centers (phase shifts) is narrower, but has a gain loss. Additionally, the partial MIMO can avoid aliasing in space when the transmitting antennas are spaced at greater than half-wavelength spacing. As scanning radar, the partial MIMO radar has smaller detection range than the phased-array radar, and the full MIMO radar has the same range as the phased-array radar.

1. INTRODUCTION

Phased-array radars operate by radiating a specific electromagnetic signal into a region and detecting targets from the echo. Many techniques have been developed for transmitting and receiving beams to accumulate target energy and reject clutter plus interference [1–8]. Recently, however, MIMO radar has drawn considerable attention for reducing vulnerability, overcoming fading effect and high space resolution [9–17]. MIMO radars transmit orthogonal electromagnetic signals rather than coherent signals in traditional phased-array radars. In MIMO receiver, a matched filterbank is used to match out these

[†] Also with Department of Communication, Engineering Institute of Armed Police, Xi'an 710086, P. R. China

signal components from the echoes. There are two kinds of MIMO radar to discuss. 1) The statistical MIMO [9, 10]. All antennas are far enough from each other so that they obtain echoes from different angles of target to combat target fades. 2) The co-located MIMO radar. For co-located transmitting and receiving antennas, the target RCS is nearly identical for all antennas. Due to orthogonal signals transmitted, no beam is obtained. But the phase differences caused by transmitting antennas along with the phase differences caused by receiving antennas can form a larger virtual array with more degrees of freedom [11, 12]. So the co-located MIMO can produce a long virtual array by a small number of antennas, which is similar to minimum redundancy array. This paper focuses on the co-located MIMO radar. In previous researches, the co-located MIMO radar is focused on better parameter identifiability [13], higher sensitivity to detect slowly moving targets [14] and waveform optimization [15]. In [16, 17], MIMO radar can improve spatial resolution compared with only the one-way beam of the phased-array radar. In fact, MIMO radars can exploit phase shifts induced by different transmitting antenna. This comparison is unfair for the phased-array radar. It is necessary to further study the relationship between the MIMO radar and the phased-array radar. This paper introduces two kinds of the co-located MIMO radars, i.e., the full MIMO and the partial MIMO, gives their performance analysis on beamwidth, gain loss and detection range, and compares them to the two-way beam of the phased-array radar.

2. SIGNAL MODEL

Consider M_t omnidirectional transmitting antennas with interelement spacing $d_t = \beta\lambda/2$, where β is integer and λ the transmitting wavelength. The receiving array consists of M_r antennas with spacing $d_r = \lambda/2$. Fig. 1 shows MIMO radar array structure. Assume that waveforms have identical bandwidth and center frequency but are temporally orthogonal. And target is far from radar with the direction θ.
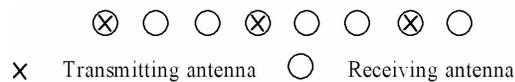

Figure 1. MIMO radar array structure.

Transmitting signal towards the target direction is represented as

$$\sum_{i=1}^{M_t} e^{-j2\pi d_t(i-1)\sin(\theta)/\lambda} s_i(n) = s(n)\mathbf{a}_t(\theta) \quad n = 1,\cdots,N \qquad (1)$$

where n denotes time, N the number of samples in time, and $s_i(n)$ the baseband signal transmitted by the ith transmitter. Denote $s(n) = [s_1(n), s_2(n), \cdots, s_{M_t}(n)]$ as the envelope sample vector of transmitting signals. $\mathbf{a}_t(\theta)$ is the transmitting steering vector, and is given by

$$\mathbf{a}_t(\theta) = \left[1, e^{-j2\pi d_t\sin(\theta)/\lambda}, \cdots, e^{-j2\pi d_t(M_t-1)\sin(\theta)/\lambda}\right]^T \qquad (2)$$

where T denotes the transpose operation. The orthogonal transmitter signals satisfy

$$\frac{1}{N}\sum_{n=1}^{N} s^H(n)s(n) = \mathbf{I}_{M_t} \qquad (3)$$

where $\mathbf{I}_{M_t}$ is an $M_t \times M_t$ identity matrix.

Let $\mathbf{x}_k(n)$ be the received signal at the kth receiver, and then $\mathbf{x}_k(n)$ can be written as

$$x_k(n) = e^{-j2\pi d_r(k-1)\sin(\theta)/\lambda}\alpha\mathbf{a}_t^H(\theta)\mathbf{s}(n) + \mathbf{w}_k(n) \qquad (4)$$

for $k = 1,\cdots,M_r$, α stands for the complex amplitude of the received signal. The received signal steering vector is given by

$$a_r(\theta) = \left[1, e^{-j2\pi d_r\sin(\theta)/\lambda}, \cdots, e^{-j2\pi d_r(M_r-1)\sin(\theta)/\lambda}\right]^T \qquad (5)$$

Denote

$$\mathbf{x}(n) = [x_1(n), x_2(n), \cdots, x_{M_r}(n)] \qquad (6)$$

as received signal vector. Combining (4) and (5), the expression (6) becomes

$$\mathbf{x}(n) = \alpha\mathbf{a}_r^*(\theta)\mathbf{a}_t^H(\theta)\mathbf{s}(n) + \mathbf{w}(n) \qquad (7)$$

where $\mathbf{w}(n) = [w_1(n), w_2(n), \cdots, w_{M_r}(n)]$ represents additive Gaussian noise vector and * stands for conjunction operation. $\mathbf{A} =$

$\mathbf{a}_t(\theta)\mathbf{a}_r^{\mathbf{T}}(\theta)$ be the two dimension transmitting-receiving steering matrix. Combining (2) and (5), yields

$$\mathbf{A} = \begin{bmatrix} 1 \\ \vdots \\ e^{-j2\pi d_r(M_r-1)\sin\theta/\lambda} \end{bmatrix} \begin{bmatrix} 1, \cdots, e^{-j2\pi d_t(M_t-1)\sin\theta/\lambda} \end{bmatrix}$$

$$= \begin{bmatrix} 1 & \cdots e^{-j2\pi d_t(M_t-1)\sin\theta/\lambda} \\ \vdots & \vdots \\ e^{-j2\pi d_r(M_r-1)\sin\theta/\lambda} & \cdots e^{j-j2\pi\{d_r(M_r-1)\sin\theta+d_t(M_t-1)\sin\theta\}/\lambda} \end{bmatrix}_{M_r\times M_t} \quad (8)$$

The received signal vector can be rewritten as

$$\mathbf{x}(n) = \alpha\mathbf{s}(n)\mathbf{A} + \mathbf{w}(n) \quad (9)$$

The temporal matched filter output of receiver is

$$\mathbf{Y} = \frac{1}{\sqrt{N}} \sum_{n=1}^{N} \mathbf{x}(n)\mathbf{s}^H(n) \quad (10)$$

where $1/\sqrt{N}s(n)$ is the matching signal vector. Here $1/\sqrt{N}$ is set so that the energy of signal would remain constant before and after matching operation.

Combining (9) and (10), we obtain

$$\mathbf{Y} = \alpha\mathbf{A} + \mathbf{E} \quad (11)$$

where $\mathbf{E} = \frac{1}{\sqrt{N}} \sum_{n=1}^{N} \boldsymbol{s}^H\boldsymbol{w}(n)$ is white noise matrix with Gauss distribution. Here assume that there is no coherence between the inference and transmitted signal.

3. BEAMFORMING

It follows from the expression (8) and (11) that the matched filter output is composed of M_tM_r signals, the number of different phase centers of which is

$$M = M_r + \beta(M_t - 1) \quad (12)$$

It means that $M_tM_r - M$ virtual overlap elements, as shown in Fig. 2. In order to ensure an uniform linear array, let $\beta \leq M_r$.
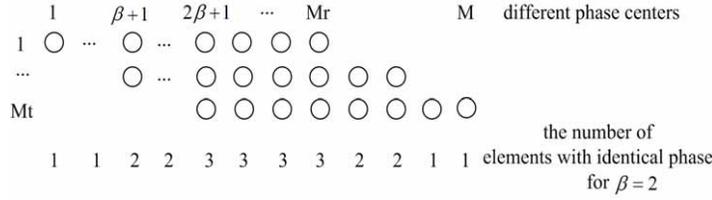
Figure 2. Virtual array structure.

If the output matrix $\mathbf{Y}$ in (11) is jointed into a $M_t M_r \times 1$ column vector, then its steering vector is $\mathbf{a}(\theta) = \mathbf{a}_t(\theta) \otimes \mathbf{a}_r(\theta)$, and the matched weight vector of the beamformer is $\mathbf{c}_{mf}(\theta_0) = \mathbf{a}_t(\theta_0) \otimes \mathbf{a}_r(\theta_0)$, where $\otimes$ indicates Kronecher product. This gives rise to the following beam pattern

$$
\begin{aligned}
P_{full}(\theta) &= \left| \mathbf{c}_{mf}^H(\theta_0)\mathbf{a}(\theta) \right|^2 \\
&= \left| \left[\mathbf{a}_t^H(\theta_0) \otimes \mathbf{a}_r^H(\theta_0) \right] \left[\mathbf{a}_t(\theta) \otimes \mathbf{a}_r(\theta) \right] \right|^2 \\
&= \left| \left[\mathbf{a}_t^H(\theta_0)\mathbf{a}_t(\theta) \right] \otimes \left[\mathbf{a}_r^H(\theta_0)\mathbf{a}_r(\theta) \right] \right|^2 \\
&= \left| \mathbf{a}_t^H(\theta_0)\mathbf{a}_t(\theta) \right|^2 \left| \mathbf{a}_r^H(\theta_0)\mathbf{a}_r(\theta) \right|^2
\end{aligned}
\tag{13}
$$

The first and second term of the above expression are transmitting and receiving beam pattern respectively. This means that MIMO radar has the same beam pattern as that of the phased-array radar. This kind of MIMO using all virtual elements is called the full MIMO. In fact, the overlap elements enhance signals at the corresponding location in the process of beamforming. Note that the number of overlap elements obeys triangle ($\beta = 1$) or ladder ($\beta > 1$) distribution along the array. This is equivalent to add a length-M window to MIMO array. For the phased-array radar, signal vectors contain a rectangular window due to limited length of transmitting or receiving array. The two-way beam (the receiving beam multiplied by transmitting one) leads to the convolution of two rectangular windows, and also produces a length-M window. Therefore, the beam pattern of the MIMO radar is identical to the two-way beam pattern of phased-array radar.

Since a rectangular window has the narrowest beamwidth of all kinds of windows, we may select elements with different phase centers to construct a length-M array. We call this kind of MIMO the partial MIMO. The difference between the full MIMO and partial MIMO depends on whether the overlap elements are utilized. The first row and last column of Y given by (11) involve all different phase centers,

and then is combined into an $M \times 1$ column vector. Its steering vector can be written as

$$\mathbf{a}_{patial}(\theta) = \left[1, e^{-j2\pi d_r \sin(\theta)/\lambda}, \cdots, e^{-j2\pi d_r(M-1)\sin(\theta)/\lambda}\right]^T \quad (14)$$

and the matched weights $\mathbf{c}_{partial}(\theta_0) = \mathbf{a}_{patial}(\theta_0)$. Then the 3-dB beamwidth is

$$\phi_{partial} \approx 0.88 \frac{\lambda}{d_M} \quad (15)$$

where $d_M = \frac{\lambda}{2}M$ is the array aperture with M elements.

If $\beta = 1$, $M_r = M_t = N$, transmitting antennas spacing is $\lambda/2$, then the number of different phase centers is $M = 2N - 1$ according to (12). So the MIMO beamwidth is

$$\phi_{partial} \approx 0.88 \frac{\lambda}{(2N-1)\frac{\lambda}{2}} \approx 0.44 \frac{\lambda}{d_N} \quad (16)$$

According to the property of the triangle (Bartlett) window [18], the two-way beamwidth of the phased-array is

$$\phi_{\text{dual}} \approx 0.64 \frac{\lambda}{d_N} \quad (17)$$

where $d_N = \frac{\lambda}{2}P$. Given $\beta = 1$, the beam pattern of the partial MIMO is a little narrower by comparing (16) to (17).

When $\beta > 1$, generally transmitting beamwidth is narrower than receiving one due to larger transmitting array aperture. In this case, the two-way beamwidth depends mainly on the transmitting beam, which is $\phi_{\text{dual}} \approx 0.88\lambda/d_{M_t}$. Since the beamwidth is inversely proportional to the array aperture, the ratio of the MIMO beamwidth to the two-way beamwidth of the phased-array radar can be computed by

$$\Upsilon = \frac{\phi_{partial}}{\phi_{\text{dual}}} = \beta M_t/[M_r + \beta(M_t - 1)] \quad (18)$$

where the expression (12) has been invoked. With β increasing, $\Upsilon \to 1$. For $\beta = M_r$, $\Upsilon = 1$ implies that the partial beamwidth is identical to the two-way one. The array gives a rectangular window. We can also get a rectangular window by setting the transmitting element spacing half wavelength and the receiving element spacing $M_t\lambda/2$.

For $\beta > 1$, there are aliasing in angle in the phased-array radar due to a sparsely sampled array. In this case, however, the partial MIMO avoids aliasing in angle because of ignoring overlap elements, which is attractive for distributed small satellite systems being researched.

4. GAIN LOSS

The partial MIMO has a narrower beam than the full MIMO. A cost on processing gain, however, has to be paid. The peak value of the beam pattern for the partial MIMO is no longer 0 dB, called gain loss. The gain loss is defined as the ratio of the gain in SNR for the partial MIMO to that for the full MIMO at the desired angle.

$$L = |P_{partial}(\theta_0)|^2 / |P_{full}(\theta_0)|^2 = \left| c_{patial}^H(\theta_0) a_{partial}(\theta_0) \right|^2 / |P_{full}(\theta_0)|^2 \tag{19}$$

Substituting (14) into the above expression, yields

$$L = M/(M_t M_r) \tag{20}$$

Substituting (12) into the above expression, we get

$$L = [M_r + \beta(M_t - 1)]/(M_t M_r) \tag{21}$$

where the range of L is $0 \leq L \leq 1$. For $\beta = M_r$, $L = 1$ implies no gain loss. For $\beta = 1$, $L = (M_r + M_t - 1)/(M_t M_r)$ reaches the minimum.

5. RADAR DETECTION RANGE

The transmitter of MIMO radar can not form the transmitting beam. Whereas, receiver can coherent a beam using phase shifts of transmitting and receiving antennas. So MIMO radar can scan a whole space and be difficult to detect. This section compares them on detection range. When radar scans a whole space, with respect to the radar range equation, the maximum detection range satisfies [19]

$$R_{Phase}^4 = \frac{P_{av} A_r t_s \sigma}{(4\pi)^2 k T_s L_s (S/N)_{\min}} \tag{22}$$

where P_{av} is average transmitting power, A_r the effective receiving area, t_s scanning time, σ RCS, k the Boltzmann constant, T_s thermal temperature, L_s total loss, $(S/N)_{\min}$ the minimum detectable SNR.

Since only M elements of $M_t M_r$ virtual elements in MIMO radar are utilized to coherent a beam, the effective aperture areas is $A_r \frac{M}{M_t M_r}$. The detection range of MIMO radar satisfies

$$R_{MIMO}^4 = \frac{P_{av} A_r t_s \sigma}{(4\pi)^2 k T_s L_s (S/N)_{\min}} \frac{M}{M_t M_r} \tag{23}$$

For the full MIMO, $M = M_t M_r$. From (22) and (23), we can find that the full MIMO has the same detecting range as the phased-array radar. This implies that during the time it takes the phased-array radar to scan the whole space, the full MIMO radar can accumulate target energy to realize the same detection range.

For the partial MIMO, $M = M_r + \beta(M_t - 1)$. Then applying to (22) and (23), we get

$$\left(R^4\right)_{MIMO} = \frac{M_r + \beta(M_t - 1)}{M_t M_r} \left(R^4\right)_{Phase} \tag{24}$$

If $\beta = 1$, $M_t = M_r = N$, then MIMO radar has the detection range as that of the phased-array radar multiplied by $\sqrt[4]{2/N}$ approximately. Obviously, although the partial MIMO has a narrow mainlobe, its detection range is smaller since not all virtual elements are utilized to accumulate target energy. It should be noted that the above comparison is based on the same scanning time for MIMO radar and the phased-array radar.

6. SIMULATION RESULTS

In this section, we consider numerical examples that compare the performances of the various systems. These examples also validate the analysis conducted in the previous sections. Consider ten transmitting antennas and ten receiving antennas, that is, $M_r = M_t = 10$. Table 1 gives the variation of array aperture with β increasing. Table 1 shows that the larger spacing for transmitting antennas, the closer the array aperture of MIMO radar becomes to that of the phased-array radar.

Figure 3 plots the beam patterns of the full, the partial MIMO and the phased-array radar for $\beta = 1$. From Fig. 3, we can see that the full MIMO beam pattern is identical to the two-way one with -26 dB peak sidelobe level. However, the partial MIMO has narrower mainlobe, but with about 7.2 dB gain loss and sidelobes with -13 dB level relative to the mainlobe peak value.

Table 1. Array apertures for deferent β.

β	1	2	3	4	5	6	7	8	9	10
Phased-array	10	20	30	40	50	60	70	80	90	100
MIMO radar	19	28	37	46	55	64	73	82	91	100

Figure 4 gives a comparison of the beam patterns of various systems for $\beta = 6$. In Fig. 4, there are ambiguities in angle for

the full MIMO radar or the two-way beam pattern of phased-array radar. These ambiguities result from sparse transmitting antennas. The partial MIMO radar avoids grating lobes and has the nearly same main lobe as the two-way one. However, we also can see that there is
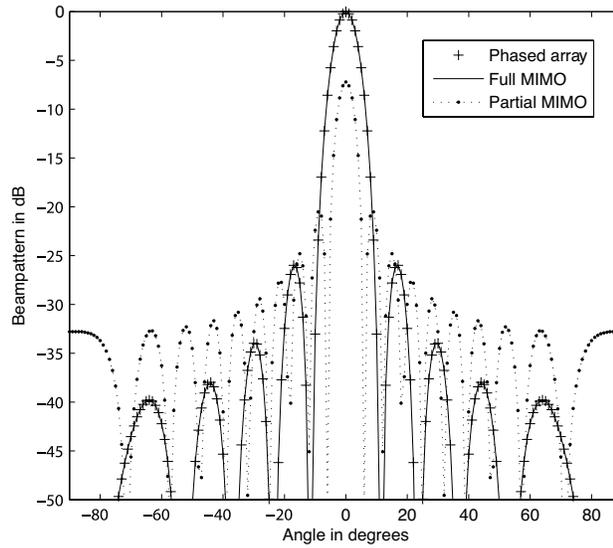

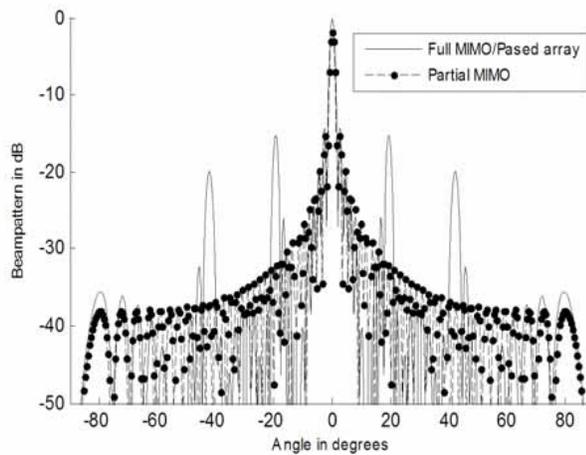**Figure 3.** Beam patterns for various systems for $\beta = 1$.

Figure 4. Beam pattern for various systems for $\beta = 6$.

about 2 dB gain loss for the partial MIMO radar.

Simulations show that the partial MIMO obtain a relatively narrow beamwidth at the cost of a relatively large gain loss and high sidelobe level.

7. CONCLUSIONS

In this paper, performances have been discussed for MIMO radar on beamforming, gain loss and detection range. MIMO radar can steer a narrow beam utilizing multiple antennas of the transmitter and the receiver. The beam pattern of the full MIMO is identical to that of the phased-array radar. However, the partial MIMO radar has narrower beamwidth with a gain loss and sidelobes with about -13 dB level. For the sparse transmitting array, the partial MIMO can avoid aliasing in space. As scanning radar, the full MIMO radar has the same detection range as phased-array radar, and the partial MIMO radar has smaller detection range. It should be pointed out that both the full and partial MIMO radars are capable of increasing the adaptive degrees of freedom, which can improve the clutter rejection for airborne radars.

ACKNOWLEDGMENT

REFERENCES

1. Rocca, P., L. Manica, and A. Massa, "An effective excitation matching method for the synthesis of optimal compromises between sum and difference patterns in planar arrays," *Progress In Electromagnetics Research B*, Vol. 3, 115–130, 2008.
2. Guney, K. and M. Onay, "Amplitude-only pattern nulling of linear antenna arrays with the use of Bees algorithm," *Progress In Electromagnetics Research*, PIER 70, 21–36, 2007.
3. Mahanti, G. K., A. Chakraborty, and S. Das, "Design of fully digital controlled reconfigurable array antennas with fixed dynamic range ratio," *Journal of Electromagnetic Waves and Applications*, Vol. 21, No. 1, 97–106, 2007.
4. Mohamed, M. A., E. A. Soliman, and M. A. El-Gamal, "Optimization and characterization of electromagnetically coupled patch antennas using RFB neural networks," *Journal of Electromagnetic Waves and Applications*, Vol. 20, No. 8, 1101–1114, 2006.

5. Babayigit, B., K. Guney, and A. Akdagli, "A clonal selection algorithm for array pattern nulling by controlling the positions of selected elements," *Progress In Electromagnetic Research B*, Vol. 6, 257–266, 2008.

6. Mouhamadou, M., P. Vaudon, and M. Rammal, "Smart antenna array patterns synthesis: Null steering and multi-user beamforming by phase control," *Progress In Electromagnetics Research*, PIER 60, 95–106, 2006.

7. Chen, T. B., Y. L. Dong, Y. C. Jiao, et al., "Synthesis of circular antenna array using crossed particle swarm optimization algorithm," *Journal of Electromagnetic Waves and Applications*, Vol. 20, 1785–1795, 2006.

8. Zhai, Y. W., X. W. Shi, and Y. J. Zhao, "Optimized design of ideal and actual transformer based on improved micro-genetic algorithm," *Journal of Electromagnetic Waves and Applications*, Vol. 21, 1761–1771, 2007.

9. Fishler, E., A. Haimovich, R. S. Blum, et al., "Performance of MIMO radar systems: Advantages of angular diversity," *Proc. 38th IEEE Asilomar Conf. on Signals, Systems, and Computers*, Vol. 1, 305–309, 2004.

10. Fishler, E., A. Haimovich, R. S. Blum, L. J. Cimini, et al., "Spatial diversity in radars-models and detection performance," *IEEE Trans. on Signal Processing*, Vol. 54, No. 3, 823–837, 2006.

11. Rabideau, D. J. and P. Parker, "Ubiquitous MIMO multifunction digital array radar," *Proc. 37th IEEE Asilomar Conf. on Signals, Systems, and Computers*, Vol. 1, 1057–1064, 2003.

12. Bliss, D. W. and K. W. Forsythe, "Multiple-input multiple-output (MIMO) radar and imaging: Degrees of freedom and resolution," *Proc. 37th IEEE Asilomar Conf. on Signals, Systems, and Computers*, Vol. 1, 54–59, 2003.

13. Li, J., P. Stoica, L. Xu, et al., "On parameter identifiability of MIMO radar," *IEEE Signal Processing Papers*, Vol. 14, No. 12, 968–971, 2007.

14. Forsythe, K., D. Bliss, and G. Fawcett, "Multiple-input multiple-output (MIMO) radar: Performance issues," *38th Asilomar Conference on Signals, Systems and Computers*, Vol. 1, 310–315, Pacific Grove, CA, November 2004.

15. Forsythe, K. W. and D. W. Bliss, "Waveform correlation and optimization issues for MIMO radar," *Proceedings of the 39th Asilomar Conference on Signals, Systems and Computers*, 1306–1310, November 2005.

16. Bekkerman, I. and J. Tabrikian, "Target detection and localization using MIMO radars and sonars," *IEEE Transactions on Signal Processing*, Vol. 5, No. 10, 3873–3883, 2006.

17. Robey, F. C., S. Coutts, and D. Weikle, "MIMO radar theory and experimental results," *Conference Record of the Thirty-Eighth Asilomar Conference on Signals, System and Computers*, Vol. 1, 300–304, 2004.

18. Manolakis, D. G., V. K. Ingle, and S. M. Kogon, *Statistical and Adaptive Signal Processing*, McGraw-Hill Companies, 2000.

19. David, K. B., *Radar System Analysis and Modeling*, Artech House Inc., 2005.